Research Article

Chemical and physical characterization of rice husk biochar and ashes and their iron adsorption capacity

Fabiane Figueiredo Severo[1] · Leandro Souza da Silva[1] · Janielly Silva Costa Moscôso[1] · Qamar Sarfaraz[2] · Luiz Fernando Rodrigues Júnior[3] · Augusto Ferreira Lopes[1] · Laura Brondani Marzari[1] · Gustavo Dal Molin[1]

Received: 17 March 2020 / Accepted: 16 June 2020 / Published online: 25 June 2020

Abstract
After flooding in rice crops, the Fe^{3+} ions from iron oxide minerals are reduced to Fe^{2+} in the anaerobic conditions, making it soluble. The excess of Fe^{2+} in soil solution can be toxic to plants, resulting in decreasing rice yield. Pyrolyzed materials from rice crop residues, such as rice husk, can be an environmentally friendly option to reduce iron availability in soil solution, provided they have appropriate chemical and physical characteristics regarding iron adsorption. In this study, rice husk biochar (RHB) and rice husk ashes (RHA1 and RHA2) were characterized regarding physical and chemical characteristics and the iron adsorption capacity. The different oxygenation conditions in obtaining the materials resulted in chemical and physical differences (e.g., biochar carbon content of 46% and ashes of 16% and 0.93%), but there were no significant differences related to iron adsorption capacity in aqueous solution. The iron adsorption capacity of the biochar was 5.53 mg Fe^{2+} g^{-1} and of the ashes was 6.74 and 7.22 mg Fe^{2+} g^{-1} for the two materials tested, which demonstrates potential of these materials to mitigate iron toxicity in flooded rice crops.

Keywords Flooded rice · Iron toxicity · Biomaterials · Organic amendments · Adsorption isotherm

1 Introduction

In flooded rice crops, the Fe^{3+} ions from iron oxide minerals are reduced to Fe^{2+} in the anaerobic conditions. The Fe^{2+} is more soluble chemical specie and, consequently, can be absorbed by rice plants, being able to cause toxicity affecting rice yield potential [1, 2]. At the same time, rice production annually generates a huge quantity of husks that can be converted into ash after burning in furnaces or boilers of grain processing industries [3]. When the rice husk is burnt under uncontrolled conditions, much of the organic matter is removed. Lignin and cellulose are oxidized, and the resulting material is composed of primarily silica (up to 95%) and other components such as iron, aluminum, calcium and potassium oxides [4] in variable quantity according to rice crop and harvest conditions, soil characteristics and methods of burning [5]. In general, rice husk ash is a material of difficult degradation, with high specific surface area, porous structure and some metal retention capacity [6].

When the organic materials are burnt in a controlled environment (i.e., temperature and time with little or no oxidation–pyrolysis), the production of biochar occurs. Biochar generally has a higher carbon content compared to ash, high CEC, high porosity and complexing ability with metals. Although biochars are obtained from biomass composed predominantly of cellulose, lignin and hemicellulose [7], other factors, such as the rate of heating and temperature and time of burning, can affect their

✉ Leandro Souza da Silva, leandrosolos@ufsm.br | [1]Department of Soils, Federal University of Santa Maria (UFSM), Roraima Avenue No. 1000 – Building 42, Santa Maria 97110-420, Brazil. [2]Department of Soil and Environmental Sciences, University of the Poonch Rawalakot-AJK, Poonch, Pakistan. [3]Department of Biomedical Engineering, Universidade Franciscana, Rua dos Andradas 1614, Santa Maria, Brazil.

characteristics even though they originate from the same type of biomass.

Ashes and biochars have been evaluated in environmental studies regarding their adsorption capacity of polluting elements or substances. The use of biochars for organic and inorganic pollutants removal from aqueous solutions has proved to be efficient for a large group of substances, such as dyes, pesticides and heavy metals [8, 9]. Studies using rice husk ash as an adsorbent material in solutions were also performed, including lead and mercury adsorption in aqueous systems [10] and the stabilization of lead and zinc [11].

The interaction of biochar and ash with heavy metals occurs with the inorganic silanols (Si–OH) groups present in ash structure or with organic functional groups, such as hydroxyls (–OH) and carboxylic acids (–COOH), including the possible presence of other functional groups from mineral oxides [12]. Recent studies evaluating adsorption of numerous metals, such as Cr, Cu, Pb, Hg, Zn and As, by activated carbon from coal also showed efficiency; however, the proper destination of the coals with adsorbed metals becomes costly. Therefore, studies with adsorptive materials obtained locally and available on a large scale without prior preparation and subsequent disposal are necessary [13].

In this context, we hypothesized that rice husk ash and/or biochar could be used as alternatives for iron toxicity mitigation in flooded rice crops, provided they have appropriate chemical and physical characteristics regarding iron adsorption. The objectives of this study were: (i) to characterize rice husk ash and biochar in relation to parameters such as elemental composition, ash content, functional groups, neutralization capacity, surface area, crystallinity degree and active sites and (ii) to evaluate the iron adsorption capacity of rice husk ash and biochar.

2 Materials and methods

2.1 Obtaining rice husk ash and biochar

Both rice husk ashes (RHA1) and (RHA2) were collected from two different rice trade companies Primo Berleze & Cia and processing of J. Fighera & Cia rice in Santa Maria, RS, respectively. Rice husks are used in furnaces to generate heat for grain processing, without controlling firing conditions (temperature or time), but RHA1 was more time exposed to the furnace than RHA2. The ash is disposed on the ground in open air, and collections were randomly carried out in piles, being packed in plastic bags for transportation and subsequent analysis. There was no pretreatment or drying done on material.

A biochar (RHB) was prepared from rice husk (collected at a rice mill in Santa Maria, RS) under slow pyrolysis conditions. The husks were pre-air-dried and then pyrolyzed for 1 h at 500 °C in a muffle furnace (Jung brand, model 7549) with 10 °C min^{-1} increase in temperature.

2.2 Chemical and physical characterization of materials

Total carbon (C) and nitrogen (N) contents of ashes/biochar were determined using an elemental analyzer (Flash model EA-1112, Thermo Scientifics). For elemental composition, 200 mg of each material was burnt in a muffle at 500 °C for 8 h and digestion was carried out with nitric acid + hydrogen peroxide [14]. Calcium (Ca), magnesium (Mg), iron (Fe), manganese (Mn), copper (Cu) and zinc (Zn) contents were measured by an atomic absorption spectrometer (AAnalyst 200—PerkinElmer), except for phosphorus (P) by using a spectrophotometer (BEL model S05) [15].

The cation exchange capacity (CEC) was determined according to Silva [16], and the neutralization power (NP) was determined by the same procedure used for lime described by Brasil [17]; however, the solutions used had to be diluted in relation to the original methodology, given the low neutralization power of the materials. Surface acid groups (carboxylic acids, phenols and lactones) were estimated by return titration as described in Boehm [18]. The ash content was determined according to ASTM D3172-13 [19]. The specific surface area (SSA) was determined by the BET procedure in an automatic determiner (Quantachrome Instruments) at the Ceramic Materials Laboratory (LACER) of the Federal University of Rio Grande do Sul (UFRGS).

The biochar and ashes samples were characterized by X-ray diffraction (X-ray diffraction DXA, Advance Bruker), after milling in mortar and pestle, sieved in 45-micron mesh and powdered in the equipment. The analyses were performed at room temperature with a copper tube ($K\alpha = 1.5418$ Å radiation), in a range of 2θ of 10°–70°, with resolution of 0.02° and 0.6 s count time. The samples were also ground in mortar and pestle, mixed with potassium bromide (KBr), pressed and characterized by Fourier transform infrared spectroscopy (FTIR) in a spectrophotometer (Spectro One model, Perkin-Elmer) to identify functional groups at the Department of Material Engineering of the Franciscan University (UFN).

The samples were also evaluated by X-ray photoelectron spectroscopy (XPS) for surface characterization (qualification and quantification of the functional group elements on the surface of the solid material), as well as determination of the content of Si and O in the samples at the Department of Inorganic Chemistry of the Federal University of Rio Grande do Sul (UFRGS). For the evaluation by

XPS, previously ground samples were placed in a spectrophotometer (Omicron-SPHERA), using an Al Kα radiation source (1486.6 eV) with an application to the anode 225 W (15 kV, 15 mA). The pressure used during the analyses was between 10^{-8} and 10^{-9} mbar. The detection angle of the photoelectrons (Θ) relative to the sample surface was set at 53° for all measurements. All binding energies on the spectra are referenced to C1s at 284.8 eV.

2.3 Iron adsorption capacity

Iron adsorption isotherms were determined using 0.5 g aliquots of previously ground triplicate sample of biochar/ash which were added to snap-cap flasks containing 50 mL of hydrated iron penta sulfate solution ($Fe_2SO_4.7H_2O$) of 0, 5, 10, 20, 40, 80 and 120 mg L^{-1} concentrations. After shaking on a horizontal shaker for 24 h at room temperature (23 °C), a 20 mL aliquot was filtered on cellulose membrane (0.2 µm) and the iron concentrations were determined by atomic absorption spectroscopy. The initial pH of the iron solution was measured and that was around 3.8. The value was fixed in this pH due to avoiding the formation of soluble iron hydroxides that occurs above pH 5.5. From the experimental data, the equations were adjusted according to the Langmuir model [20]. The main idea was to use a model that can give an estimation of a maximum iron adsorption capacity to compare the biochar and ashes, and we believe that it was appropriate using Langmuir equations in our study.

$$Q = \frac{K_L \times C_{max} \times C_{sol}}{1 + K_L \times C_{sol}} \quad (1)$$

where Q = amount of Fe^{2+} in equilibrium; C_{max} = maximum sorption capacity of Fe^{2+}; K_L (Langmuir's constant) = constant related to the affinity of the biochar/ash for Fe^{2+}; C_{sol} = concentration of Fe^{2+} in the solution.

The parameter C_{max} is related to the maximum adsorption capacity and K_L is the ratio between the adsorption kinetic constant and kinetic desorption constant [21]. The separation factor (RL) was also calculated. This parameter is used to predict the nature of adsorption (spontaneity) and is defined according to the equation [22]:

$$RL = \frac{1}{1 + K_L.C_{max}}. \quad (2)$$

If RL > 1, isotherm is unfavorable; if RL = 1, isotherm is linear; and if 0 < RL < 1, isotherm is favorable.

A sample of the ashes and biochar used in the isotherm experiment was oven-dried (60 °C) up to constant weight for evaluation by XPS by the same procedure described above.

2.4 Statistical analysis

The values obtained in the nutrient analyses of the ashes and the biochar were submitted to analysis of variance (ANOVA), and when necessary, the means comparison was performed by the Tukey test (5% level of significance).

3 Results

3.1 Chemical and physical characterization of materials

The RHB presented higher C content, followed by RHA1 and RHA2 (Table 1). Virtually, no N was detected in ashes, while a low concentration still persisted in biochar. Unlike C and N, higher Si content was verified in both ashes. There was no significant difference in Mn, Mg, Ca, Cu, Fe, K and P contents among materials, which are in relatively low concentrations, except for *P* and *K*, which presented higher values compared to the others. The materials presented low neutralization power (NP), although different from each other (Table 1). A higher CEC value was obtained in the RHB compared to the ashes. The presence of carboxylic radicals (–COOH) in the materials was not detected. The phenolic groups (–OH) were higher in relation to the lactonic groups (–COOR) in biochar and ashes.

The functional groups present in biochar and ashes evaluated by FTIR are very similar to each other (Fig. 1). The transmittance peak between 3678 and 3272 cm^{-1} present in three materials indicates the presence of hydroxyl groups (–OH). These groups may be derived from phenols, alcohols, ethers and esters. In all materials, the peak in 1617 cm^{-1} shows the stretch related to aldehydes. Stretches occurring at 1092, 1,097 and 1,095 cm^{-1} (for RHB, RHA1 and RHA2, respectively) confirm the presence of silanols (Si–OH) and siloxanes (Si–O–Si–OH) groups. In addition, a specific peak (793 cm^{-1}) for Si–H in these materials was also verified.

The three materials showed silicate structures in several crystalline arrangements (cristobalite, quartz and morganite) in the XRD evaluation (Fig. 2). It was possible to verify the presence of four mineral crystalline phases in the biochars diffractogram (RHB), including one containing Ca (Fig. 2a). Besides the identification of the silicate phases, diffractogram from biochar has a diffuse baseline, with no predominant peaks, characteristic of large amounts of amorphous components in its composition. In RHA1, occurrence of silicate phases (quartz and cristobalite) was also verified, as well as the presence of Ca in its crystalline structure (gyrolineite). The RHA2 presented phases with the presence of silica (cristobalite) and K.

Table 1 Chemical and physical parameters of rice husk biochar (RHB) and ashes (RHA1 and RHA2)

Chemical and physical parameters	RHB (mean value ± SD[c])	RHA1 (mean value ± SD)	RHA2 (mean value ± SD)
Carbon (%)	46,1 ± 2,05 *a*	0,93 ± 0,05 *c*	16,5 ± 2,11 *b*
Nitrogen (%)	0,43 ± 0,02 *a*	< 0,01b	0,01 *b*
Oxygen (%)	19,5 ± 2,1 *b*	26,5 ± 2,1 *a*	14,5 ± 1,7 *c*
Silicon (%)	35,0 ± 4,2 *c*	66,0 ± 8,5 *a*	59,5 ± 7,8 *b*
Manganese (g kg^{-1})	0,55 ± 0,11	0,32 ± 0,04	0,45 ± 0,11
Magnesium (g kg^{-1})	0,50 ± 0,03	1,09 ± 0,43	0,69 ± 0,08
Calcium (g kg^{-1})	0,81 ± 0,04	1,28 ± 0,53	1,00 ± 0,01
Cooper (g kg^{-1})	< 0,01	0,03 ± 0,02	0,01
Zinc (g kg^{-1})	0,08 ± 0,01 *a*	0,13 ± 0,01 *b*	0,12 ± 0,01 *b*
Iron (g kg^{-1})	0,24 ± 0,01	0,37 ± 0,10	0,34 ± 0,04
Potassium (g kg^{-1})	5,1 ± 0,13	6,2 ± 1,81	5,3 ± 0,37
Phosphorus (g kg^{-1})	1,2 ± 0,09	3,1 ± 0,70	2,5 ± 1,29
Ash (%)	35,4 ± 0,35 *a*	96,0 ± 0,15 *b*	68,9 ± 1,44 *c*
Neutralizing power (%)	0,76 ± 0,01 *a*	0,51 ± 0,02 *b*	0,44 ± 0,04 *c*
Carboxylic groups ($mmol_c$ g^{-1})	< 0,01	< 0,01	< 0,01
Lactonic groups ($mmol_c$ g^{-1})	3,5 ± 0,31 *b*	4,5 ± 0,2 *a*	2,7 ± 0,2 *c*
Phenolic groups ($mmol_c$ g^{-1})	31,0 ± 2,2 *a*	6,2 ± 0,2 *c*	9,5 ± 0,2 *b*
CEC[a] ($cmol_c$ kg^{-1})	112,5 ± 2,5 *a*	40,0 ± 5 *c*	57,5 ± 2,5 *b*
SSA[b] (m^2 g^{-1})	118,2 ± 2,38 *a*	9,2 ± 0,24 *c*	9,5 ± 1,18 *bc*

Means followed by distinct letters in horizontal line have significant differences according to the Tukey's test ($p < 0.05$)

[a]Cation exchange capacity

[b]Specific surface area

[c]Standard deviation

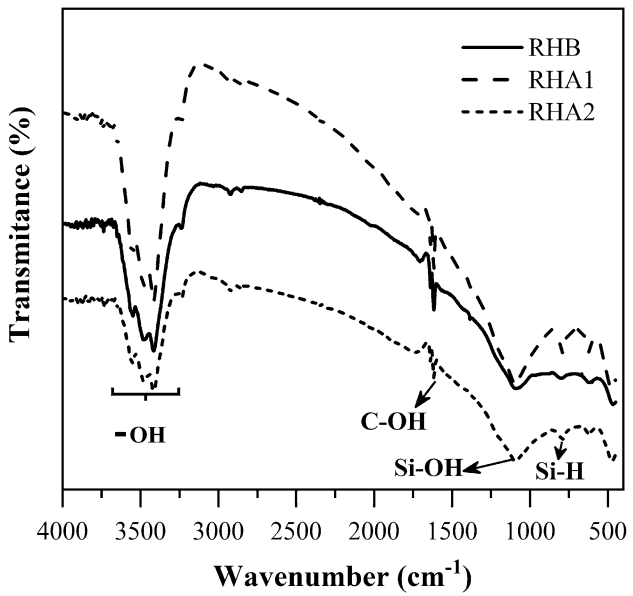

Fig. 1 Transmittance spectrum obtained by Fourier transform infrared (FTIR) biochar (RHB) and ashes (RHA1 and RHA2) of rice husks

The photoelectric spectrum obtained by XPS evaluation of the biochar surface (RHB) and ashes (RHA1 and RHA2) evidenced presence of O, C, Si and Ca (Fig. 3). The spectral lines of O (O1s) for RHB showed binding energy equal to 533.9 eV, and this is related to the presence of C = O type bonds, which confirms previously obtained information in FTIR evaluation and indicates presence of surface groups in the biochar such as phenols, ethers and hydroxyls. Carboxylic groups were previously discarded by Boehm method (Table 1). For ashes RHA1 and RHA2, value found was 532.8 eV and can be related to the presence of O to Si in the SiO_2 form.

The XPS spectral line of Ca (Ca2p) had binding energy of 347.8 eV for all materials, and this value is related to presence of $Ca_3(PO_4)_2$ in the three materials (Fig. 3). The spectral line of Ca was also present as Ca3p and binding energy of 26.8 eV, a value that relates the presence of Ca oxide in the biochar. The spectral line of C (C1s), whose binding energy was 284.8 eV in all materials tested, indicates that this element also carries out single bonds (sp3-type hybridization), fact previously confirmed by FTIR (stretches of type CH aliphatic). The spectral line of Si occurred under two binding energies (Si2s and Si2p). The binding energy values for Si2s were around 155.4 eV in the three materials and refer to Si in inorganic form (SiO_2).

The XPS evaluation was also performed on the materials after exposure to the Fe^{2+} ions in the adsorption isotherm (Fig. 4). The binding energy values of elements O,

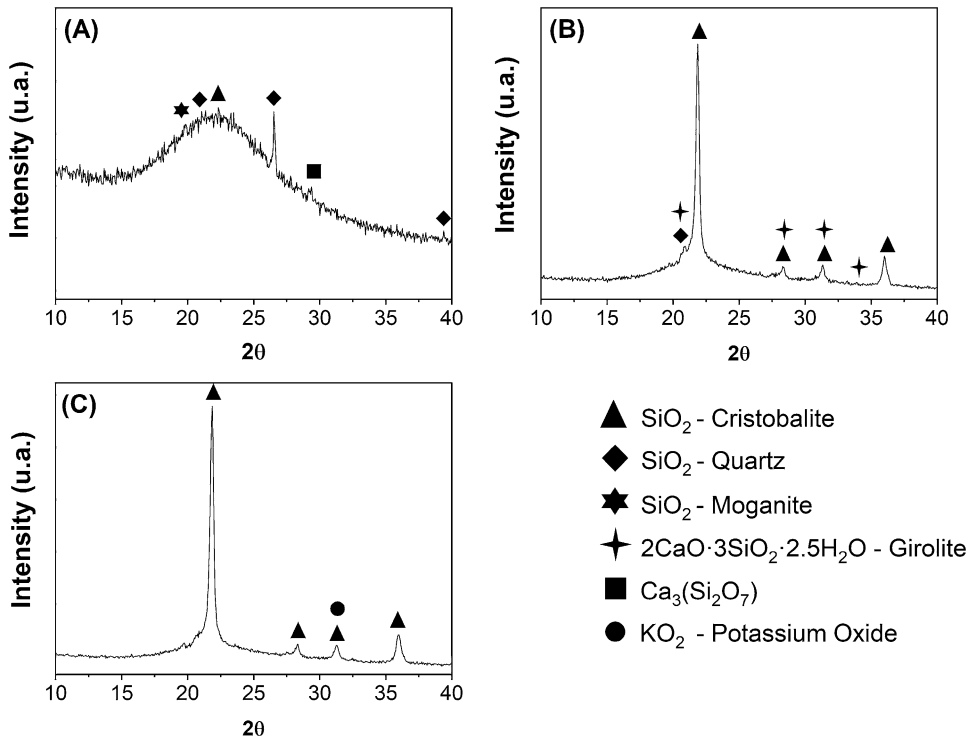

Fig. 2 X-ray diffraction of **a** biochar (RHB) and ashes **b** RHA1 and **c** RHA2 of rice husks

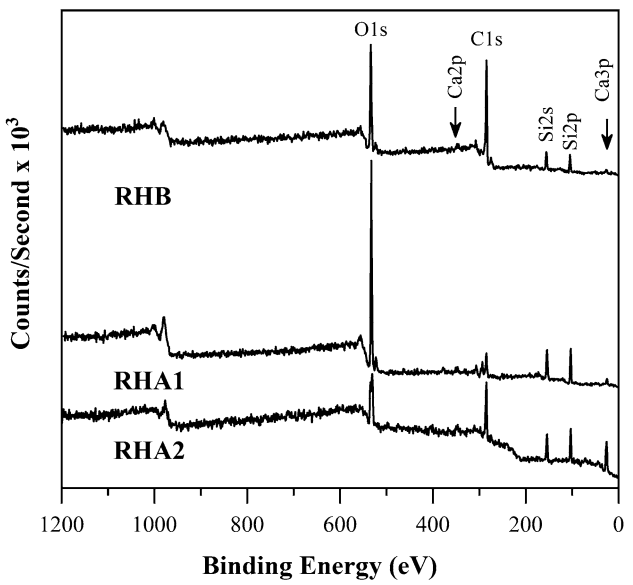

Fig. 3 Photoelectric spectrum (XPS) of rice husk biochar (RHB) and ashes (RHA1 and RHA2) surfaces

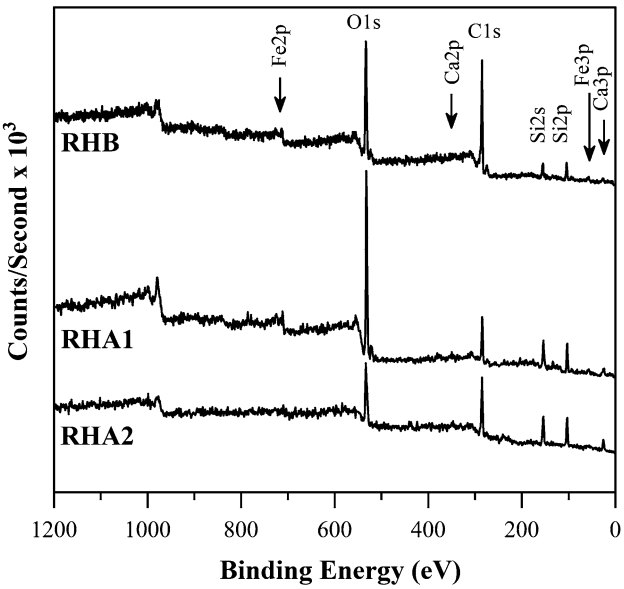

Fig. 4 Photoelectric spectrum (XPS) of the biochar surface (RHB) and ashes (RHA1 and RHA2) of rice husk after eight days of contact with solution containing Fe^{2+} ions

Ca, C, Si and Ca remained the same. By means of deconvolution, it was possible to verify in a more detailed way different binding energies that compose peak formed in the primary region for the element Fe (Fe2p) (Fig. 5). There are the presences of $FeSi_2$, FeSi, and Fe_3Si (707.2 eV, 707 eV and 706.8 eV, respectively), of Fe–$FeSO_4$ (711–713 eV), and of the bindings of Fe^{2+} in the oxide form (709.1 eV, 709.8 eV and 710.6 eV).

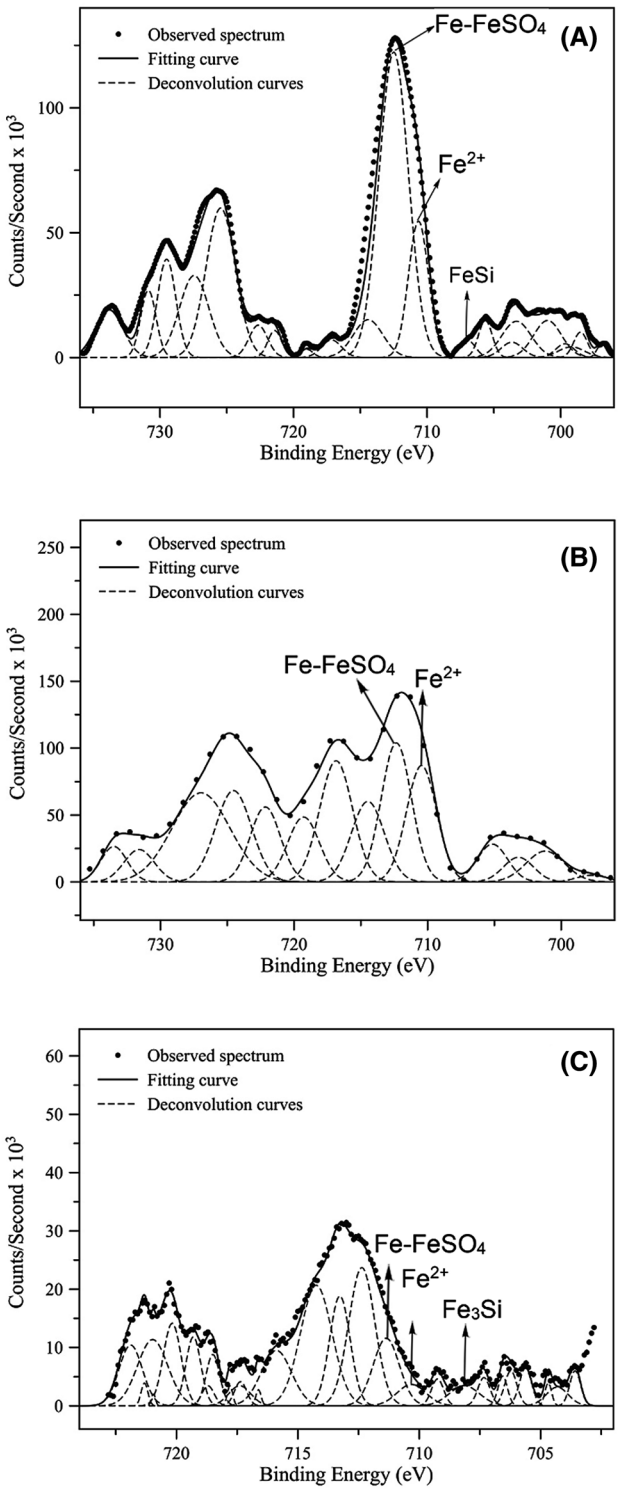

Fig. 5 Deconvolution of Fe2p primary region in XPS spectrum of **a** biochar (RHB) and ashes **b** RHA1 and **c** RHA2 of rice husk after eight days of contact with Fe^{2+} solution

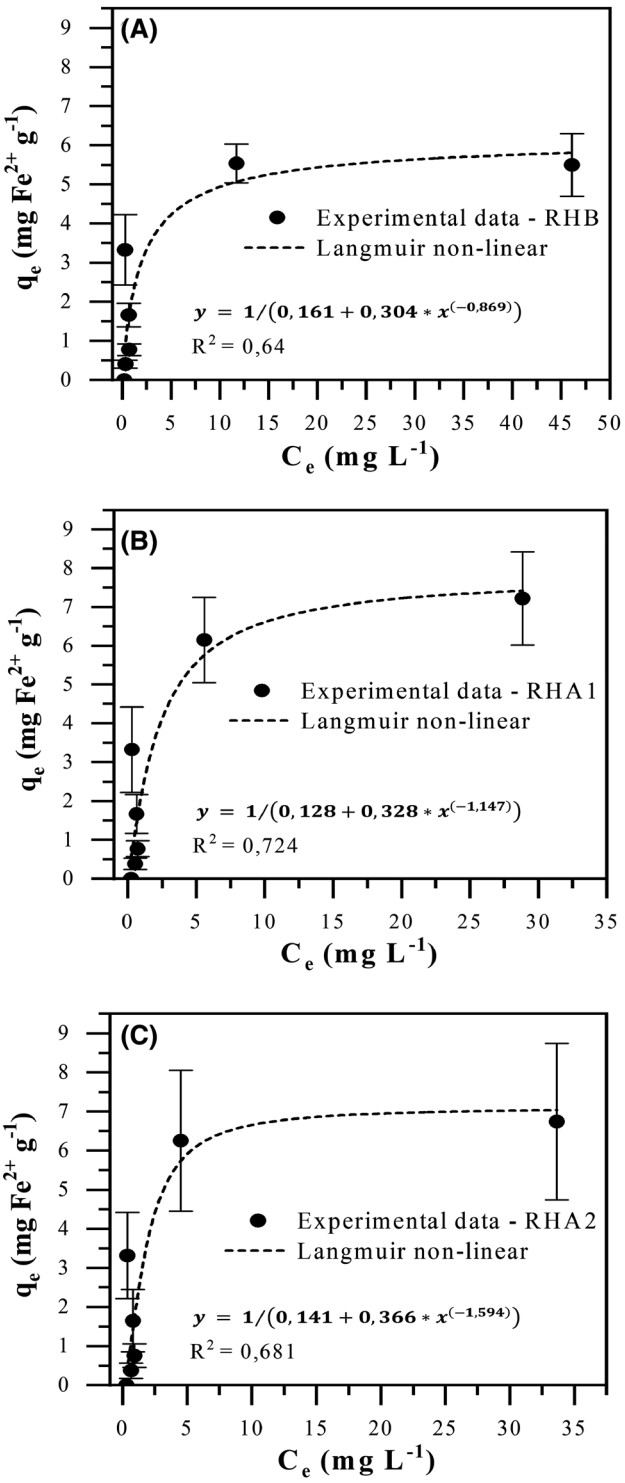

Fig. 6 Iron adsorption isotherms in **a** biochar (RHB) and ashes **b** RHA1 and **c** RHA2 of rice husk adjusted by the Langmuir equation. Error bars represent the standard deviation

3.2 Iron adsorption capacity

The iron adsorption capacity was determined by isotherms (Fig. 6). The Langmuir constant (KL), which indicates the adsorption affinity of adsorbate by adsorbent, also presented close values between the materials (0.10 mg L^{-1}, 0.10 mg L^{-1} and 0.14 mg L^{-1} for RHB, RHA1 and RHA2, respectively), indicating similar affinity of these materials for iron. For the separation factor (RL), values found for RHB (0.7) and RHA1 and RHA2 (0.8) denote the occurrence of favorable and spontaneous iron adsorption. The maximum adsorption capacities of RHB, RHA1 and RHA2 were 5.53, 7.22 and 6.74 mg Fe^{2+} g^{-1}, respectively.

4 Discussion

4.1 Chemical and physical characterization of materials

The differences regarding C content in RHB, RHA1 and RHA2 were expected because of the higher oxygenation during ash production, guaranteeing greater carbon oxidation conditions converting organic carbon to CO_2. The higher P and K contents in the biochar and ashes compositions justify their fertilizer effects on soil and plant uptake [23, 24]. Regarding lower values of NP, the study of Islabão [3] also showed a very low NP (0.91%) for rice husk ashes and the application of them can cause a significant increase in the soil pH only at doses above 40 Mg ha^{-1}. Although higher soil pH can decrease Fe^{2+} in soil solution during flooded rice crops, rice husk ashes cannot be considered a viable alternative to replacing limestone for raising soil pH due to the large amount required to be applied. Although it is not as common to reach CEC values as high as that obtained for biochars in this study (112.5 $cmol_c$ kg^{-1}), studies with biochar from cane residues found values close to 120 $cmol_c$ kg^{-1} [25]. CEC can be very variable among different biochars, since it depends directly on temperature of production and the feedstock [26]. The lower CEC of ashes may be related to lower SSA, similar to those found in other studies [23]. However, SSA can be strongly affected by temperature or chemical activation using potassium hydroxide in desiccated coconut residue as agricultural waste materials [35, 36].

Although a greater number of phenolic groups in the biochar are expected due to pyrolysis condition, there was no expectation to be found in the ashes, especially RHA1, due to the lower amount of carbon. However, the Boehm method [18] is usually used in higher carbon materials, and because of this, the methodology may present limitations for ashes characterization. As the principle involves an indirect estimate, other inorganic functional groups (e.g., silicates) may influence the results.

The results found by FTIR are very similar to those found in studies evaluating ashes and biochars from rice husk [23, 24]. The presence of organic functional groups described, as well as presence of silanols and siloxanes in ash, is responsible for ability of these materials to adsorb metals [23]. It was possible to identify possible CH stretches of aliphatic (2,923 and 2,850 cm^{-1}), stretches of –C = O and –C–OH from ketones and aldehydes (1,636 and 1,615 cm^{-1}), stretches of oxygen groups typical of lignin (1,200 cm^{-1}) and metals such as K and Ca (620 cm^{-1}) [24, 27]. However, it is necessary to take into account that FTIR results have a qualitative evaluation, not expressing the amount of the functional groups in the biochar and ashes. Hence, the amount of these groups can directly affect iron adsorption capacity of these materials.

Most of the studies with XRD that have evaluated rice-derived biochars converge to the appearance of peaks related to SiO_2 structures represented in various arrangements and with elements such as Ca and K [24]. The formation of crystalline phases in the biochar is usually related to obtaining this material at high temperatures (700 to 800 °C), but this was also substantiated in studies where this material was obtained at 500 °C [28]. Studies have shown that peaks of minerals with Ca increase at temperatures of up to 500 °C, but decrease and even disappear at higher temperatures (700–800 °C). In general, the appearance of crystalline structures containing Ca in biochars also depends on the biomass from which they were obtained. The study of Srivastava [23] also reported the presence of SiO_2 in the form of cristobalite and compounds with the presence of K in crystalline phase of rice husk ash. Therefore, when comparing ash, it is possible to affirm that firing conditions of the first one (RHA1) were more propitious to the formation of crystalline structures in relation to the second ash (RHA2). However, RHA2 ash did not present peaks related to the presence of quartz in its diffractogram. It is important to point out that the visualization of amorphous structures by this technique is not possible, which does not exempt such structures from actively participating in ion adsorption reactions.

In both ashes, the XPS value around 25.3 eV refers to this element in the form of carbonate [29]. The values in Si2p were recorded only in RHB and RHA1 (104 and 102 eV, respectively) and confirmed the presence of Si in the form of SiO_2 and amorphous silicon (SiC_xO_y) [30]. The clusters found by XPS for the rice bark derived biochar are in agreement with other studies [9], in addition to being very similar to those observed by FTIR. This reinforces the need for use of analytical techniques that complement each other in order to confirm functional groups are on surfaces of materials in characterization studies. The main difference observed in

photoelectric spectrum of these materials after exposure to the Fe^{2+} ions in the adsorption isotherm was the appearance of Fe-related bonding energies in the Fe2p and Fe3p regions, evidencing the Fe^{2+} sorption of the solution in the biochar and the ashes tested. The less intense binding values (Fe3p) are related to the appearance of Fe in $FeSO_4.7H_2O$ form [31].

By means of deconvolution of XPS, the spectral lines of Fe (Fe2p1/2 and Fe2p3/2) found in a value close to 710 eV denote the presence of this oxygen-bound element (Fe_2O_3) [32]. However, it is necessary to point out that such a structure can be adsorbed in both organic groups and in silicate structures, provided there is an electrically favorable site for this phenomenon to occur. The less intense line of Fe (Fe3p) also refers to the same structure (Fe_2O_3) found for the other peaks of the element [31]. In general, the results obtained in this study indicate potential adsorption capacity of iron by ash and biochar but involving different functional groups.

4.2 Iron adsorption capacity

The ashes have a similar adsorption isotherm to biochar (RHB). In general, three isotherms obtained can be classified as being type L (Langmuir—subgroup 2). According to classification of Giles [33], the isotherms have an initial downward curvature due to a decrease in availability of active sites. It also indicates that there was saturation of the surface at which adsorbate has more affinity for solvent than for the already adsorbed molecules. However, the adsorption of Fe to biochar and to ashes must have occurred by different functional groups and mechanisms that together ended up providing similar total capacity values, even with the biochar having the possibility of a greater retention. Studies of the iron adsorption by biochar derived from rice husks are scarce; however, when these materials are used for other metals adsorption, such as cadmium and nickel, it is possible to verify that the results are also significant [34].

Considering parameters evaluated in characterization of materials together with adsorption results evaluated in solution, it was possible to consider that rice husk biochar and ashes have different characteristics, but a similar Fe^{2+} adsorption capacity. Further studies are necessary to evaluate their addition in rice crops as an economically viable and ecologically correct alternative to minimize or even eliminate the effects of iron toxicity.

5 Conclusion

Biochar and ash of rice husk have different levels of C, Si, CEC, SSA and some characteristics of the main surface functional groups, which should be related to the difference in oxygenation and temperature during the pyrolysis of the materials. However, these differences did not result in a large difference in adsorption capacity of Fe^{2+} ions. The iron adsorption capacity of the biochar was 5.53 mgFe^{2+} g^{-1} and of the ashes was 6.74 and 7.22 mg Fe^{2+} g^{-1} for the two materials tested, which demonstrates potential of these materials to mitigate iron toxicity in flooded rice crops.

Acknowledgement The authors gratefully acknowledge all students and staff from UFSM, UFN and UFRGS on their contributions in the development of this research.

Authors' contributions FFS and LSS designed the experiment. FFS, JSCM, QS, AFL, LBM and GDM performed the experiment and analysis in the laboratory. FFS, LSS and FFRJ performed interpretation and statistical analyses of the data. FFS and LSS prepared the manuscript.

Funding This study was financed (grant and scholarships) by CNPq (National Council for Scientific and Technological Development from Brazilian government), FAPERGS (Fundação de Amparo à Pesquisa do Estado do Rio Grande do Sul), and CAPES (Coordination of Superior Level Staff Improvement from Brazilian government)—Finance Code 001.

Compliance with ethical standards

Conflicts of interest The authors declare no conflict of interest.The founding sponsors had no role in the design of the study; in the collection, analyses or interpretation of data; in the writing of the manuscript; and in the decision to publish the results. Federal University of Santa Maria—UFSM (Brazil) publishes the text and data in open access as a student's PhD thesis of Fabiane F. Severo concluded at UFSM in 2019 without conflict of interest. The authors are responsible for appropriate permissions from Primo Berleze & Cia and J. Fighera & Cia companies for rice sample collection in this study.

Availability of data and material The text and data from this manuscript are published in open access as a student's PhD thesis of Fabiane F. Severo concluded at Federal University of Santa Maria (Brazil) in 2019 (https://repositorio.ufsm.br/bitstream/handle/1/19379/TES_PPGCS_2019_SEVERO_FABIANE.pdf?isAllowed=y&sequence=1).

References

1. Wolter RCD (2010) Prognóstico da toxidez de ferro em arroz irrigado por alagamento através da análise de solo pelo método oxalato de amônio,Universidade Federal de Pelotas. https://hdl.handle.net/123456789/1184. Accessed 15 June 2016
2. Schmidt F, Fortes MÁ, Wesz J, Buss GL, Sousa RO (2013) Impacto do manejo da água na toxidez por ferro no arroz irrigado por alagamento. Rev Bras CiêncDo Solo 37:1226–1235. https://doi.org/10.1590/S0100-06832013000500012
3. IRGA—Instituto Rio Grandense do Arroz, Safra 2018/19—produção por município, (n.d.). https://www.irga.rs.gov.br. Accessed 1 June 2019
4. da Silva LB (2016) Emprego de adsorventes oriundos da casca de arroz na remoção de cobre em efluentes aquosos, Universidade Federal da Bahia. https://repositorio.ufba.br/ri/handle/ri/19132. Accessed 5 June 2019

5. Islabão GO (2013) Uso da cinza de casca de arroz como corretivo e condicionador do solo, Universidade Federal de Pelotas. https://guaiaca.ufpel.edu.br:8080/handle/123456789/2438. Accessed 21 June 2016
6. Della V, Kühn I, Hotza D (2002) Rice husk ash as an alternate source for active silica production. Mater Lett 57:818–821. https://doi.org/10.1016/S0167-577X(02)00879-0
7. Santos RB, Hart P, Jameel H, Chang H (2013) Wood based lignin reactions important to the biorefinery and pulp and paper industries. BioResources. https://doi.org/10.15376/biores.8.1.1456-1477
8. Santos H, Junger DL, Soares AB (2015) Cascas de Arroz: Uma alternativa promissora. Orbital Electron J Chem 6:267–275. https://doi.org/10.17807/orbital.v6i4.612
9. Tan X, Liu Y, Zeng G, Wang X, Hu X, Gu Y, Yang Z (2015) Application of biochar for the removal of pollutants from aqueous solutions. Chemosphere 125:70–85. https://doi.org/10.1016/j.chemosphere.2014.12.058
10. Feng Q, Lin Q, Gong F, Sugita S, Shoya M (2004) Adsorption of lead and mercury by rice husk ash. J Colloid Interface Sci 278:1–8. https://doi.org/10.1016/j.jcis.2004.05.030
11. Bosio A, Zacco A, Borgese L, Rodella N, Colombi P, Benassi L, Depero LE, Bontempi E (2014) A sustainable technology for Pb and Zn stabilization based on the use of only waste materials: a green chemistry approach to avoid chemicals and promote CO2 sequestration. Chem Eng J 253:377–384. https://doi.org/10.1016/j.cej.2014.04.080
12. Ahmad M, Rajapaksha AU, Lim JE, Zhang M, Bolan N, Mohan D, Vithanage M, Lee SS, Ok YS (2014) Biochar as a sorbent for contaminant management in soil and water: a review. Chemosphere 99:19–33. https://doi.org/10.1016/j.chemosphere.2013.10.071
13. Mohan D, Sarswat A, Ok YS, Pittman CU (2014) Organic and inorganic contaminants removal from water with biochar, a renewable, low cost and sustainable adsorbent—a critical review. Bioresour Technol 160:191–202. https://doi.org/10.1016/j.biortech.2014.01.120
14. Enders A, Hanley K, Whitman T, Joseph S, Lehmann J (2012) Characterization of biochars to evaluate recalcitrance and agronomic performance. Biores Technol 114:644–653. https://doi.org/10.1016/j.biortech.2012.03.022
15. Murphy J, Riley JP (1962) A modified single solution method for the determination of phosphate in natural waters. Anal Chim Acta 27:31–36. https://doi.org/10.1016/S0003-2670(00)88444-5
16. da Silva FC (2009) Manual de análises químicas de solos, plantas e fertilizantes, 2nd edn. Embrapa Informação Tecnológica, Brasília
17. Brasil. Ministério da Agricultura, Pecuária e Abastecimento (2017) Manual de métodos analíticos oficiais para fertilizantes minerais, orgânicos, organominerais e corretivos, MAPA, Brasília. https://www.gov.br/agricultura/pt-br/assuntos/laboratorios/legislacoes-e-metodos/fertilizantes-substratos/manual-de-metodos
18. Boehm HP (1994) Some aspects of the surface chemistry of carbon blacks and other carbons. Carbon N Y 32:759–769. https://doi.org/10.1016/0008-6223(94)90031-0
19. American Society for Testing and Materials (ASTM) (2013) ASTM D3172-13—Standard practice for proximate analysis of coal and coke. Annual Book of Standards, v. 5, 2013
20. Sparks DL (2003) Environmental soil chemistry, 2nd edn. Elsevier, San Diego. https://doi.org/10.1016/B978-0-12-656446-4.X5000-2
21. Choy KKH, McKay G, Porter JF (1999) Sorption of acid dyes from effluents using activated carbon. Resour Conserv Recycl 27:57–71. https://doi.org/10.1016/S0921-3449(98)00085-8
22. Sivaraj R, Namasivayam C, Kadirvelu K (2001) Orange peel as an adsorbent in the removal of Acid violet 17 (acid dye) from aqueous solutions. Waste Manag 21:105–110. https://doi.org/10.1016/S0956-053X(00)00076-3
23. Srivastava VC, Mall ID, Mishra IM (2006) Characterization of mesoporous rice husk ash (RHA) and adsorption kinetics of metal ions from aqueous solution onto RHA. J Hazard Mater 134:257–267. https://doi.org/10.1016/j.jhazmat.2005.11.052
24. Wu W, Yang M, Feng Q, McGrouther K, Wang H, Lu H, Chen Y (2012) Chemical characterization of rice straw-derived biochar for soil amendment. Biomass Bioenerg 47:268–276. https://doi.org/10.1016/j.biombioe.2012.09.034
25. Lu K, Yang X, Gielen G, Bolan N, Ok YS, Niazi NK, Xu S, Yuan G, Chen X, Zhang X, Liu D, Song Z, Liu X, Wang H (2017) Effect of bamboo and rice straw biochars on the mobility and redistribution of heavy metals (Cd, Cu, Pb and Zn) in contaminated soil. J Environ Manage 186:285–292. https://doi.org/10.1016/j.jenvman.2016.05.068
26. Jiang T-Y, Jiang J, Xu R-K, Li Z (2012) Adsorption of Pb(II) on variable charge soils amended with rice-straw derived biochar. Chemosphere 89:249–256. https://doi.org/10.1016/j.chemosphere.2012.04.028
27. Wang J, Xiong Z, Kuzyakov Y (2016) Biochar stability in soil: meta-analysis of decomposition and priming effects. GCB Bioenergy 8:512–523. https://doi.org/10.1111/gcbb.12266
28. de Aguiar MRMP, Novaes AC, Guarino AWS (2002) Remoção de metais pesados de efluentes industriais por aluminossilicatos. Quim Nova 25:1145–1154. https://doi.org/10.1590/S0100-40422002000700015
29. Sosulnikov MI, Teterin YA (1992) X-ray photoelectron studies of Ca, Sr and Ba and their oxides and carbonates. J Electron Spectros Relat Phenomena 59:111–126. https://doi.org/10.1016/0368-2048(92)85002-O
30. Krummacher S, Sarma DD (1986) XPS studies of the oxidation of U-Si compounds. Surf Sci 178:842–849. https://doi.org/10.1016/0039-6028(86)90359-6
31. Descostes M, Mercier F, Thromat N, Beaucaire C, Gautier-Soyer M (2000) Use of XPS in the determination of chemical environment and oxidation state of iron and sulfur samples: constitution of a data basis in binding energies for Fe and S reference compounds and applications to the evidence of surface species of an oxidized py. Appl Surf Sci 165:288–302. https://doi.org/10.1016/S0169-4332(00)00443-8
32. Zhang X, Wang H, He L, Lu K, Sarmah A, Li J, Bolan NS, Pei J, Huang H (2013) Using biochar for remediation of soils contaminated with heavy metals and organic pollutants. Environ Sci Pollut Res 20:8472–8483. https://doi.org/10.1007/s11356-013-1659-0
33. Giles CH, D'Silva AP, Easton IA (1974) A general treatment and classification of the solute adsorption isotherm part. II. experimental interpretation. J. Colloid Interface Sci. 47:766–778. https://doi.org/10.1016/0021-9797(74)90253-7
34. Deng Y, Huang S, Laird DA, Wang X, Meng Z (2019) Adsorption behaviour and mechanisms of cadmium and nickel on rice straw biochars in single-and binary-metal systems. Chemosphere 218:308–318. https://doi.org/10.1016/j.chemosphere.2018.11.081
35. Yahya MA, Al-Qodah Z, Ngah CWZCW, Hashim MA (2015) Preparation and characterization of activated carbon from desiccated coconut residue by potassium hydroxide. Asian J Chem 27(6):2331–2336. https://doi.org/10.14233/ajchem.2015.18804
36. Yahya MA, Ngah CWZCW, Hashim MA, Al-Qodah Z (2016) Preparation of activated carbon from desiccated coconut residue by chemical activation with NaOH. J Mater Sci Res 5(1):24–31. https://doi.org/10.5539/jmsr.v5n1p24